

Recognition of Host Proteins by Helicobacter Cysteine-Rich Protein C

Journal Article**Author(s):**

Roschitzki, Bernd; Schauer, Stefan; Mittl, Peer R.E.

Publication date:

2011-09

Permanent link:

<https://doi.org/https://doi.org/10.3929/ethz-b-000039242>

Rights / license:

[In Copyright - Non-Commercial Use Permitted](#)

Originally published in:

Current Microbiology 63(3), <https://doi.org/10.1007/s00284-011-9969-2>

Recognition of Host Proteins by Helicobacter Cysteine-Rich Protein C

Bernd Roschitzki · Stefan Schauer ·
Peer R. E. Mittl

Received: 8 April 2011 / Accepted: 11 June 2011 / Published online: 7 July 2011
© Springer Science+Business Media, LLC 2011

Abstract Tetratricopeptide- and sel1-like repeat (SLR) proteins modulate various cellular activities, ranging from transcription regulation to cell-fate control. Helicobacter cysteine-rich proteins (Hcp) consist of several SLRs that are cross-linked by disulfide bridges and have been implicated in host/pathogen interactions. Using pull-down proteomics, several human proteins including Nek9, Hsp90, and Hsc71 have been identified as putative human interaction partners for HcpC. The interaction between the NimA-like protein kinase Nek9 and HcpC has been validated by ELISA and surface plasmon resonance. Recombinant Nek9 is recognized by HcpC with a dissociation constant in the lower micromolar range. This interaction is formed either directly between Nek9 and HcpC or via the formation of a complex with Hsc71. The HcpC homologue HcpA possesses no affinity for Nek9, suggesting that the reported interaction is rather specific for HcpC. These results are consistent with previous observations where Nek9 was targeted upon bacterial or viral invasion. However, further experiments will be required to show that the reported interactions also occur in vivo.

Electronic supplementary material The online version of this article (doi:10.1007/s00284-011-9969-2) contains supplementary material, which is available to authorized users.

B. Roschitzki · S. Schauer
Functional Genomics Center Zurich, UZH / ETH Zürich,
Winterthurerstr. 190, 8057 Zürich, Switzerland
e-mail: bernd.roschitzki@fgcz.uzh.ch

S. Schauer
e-mail: schauer@fgcz.ethz.ch

P. R. E. Mittl (✉)
Department of Biochemistry, University of Zürich,
Winterthurer Str. 190, 8057 Zürich, Switzerland
e-mail: mittl@bioc.uzh.ch

Abbreviations

Mbp Maltose binding protein
TFA Trifluoroacetic acid
DTT Dithiothreitol
BSA Bovine serum albumine
TCEP Tris(2-carboxyethyl)phosphine

Introduction

Molecular activity, thermodynamic stability, and structural integrity of proteins are often modulated by the binding of specialized protein–protein interaction modules, such as tetratricopeptide repeat (TPR) or other repeat proteins. Sel1-like repeat proteins (SLR) have initially been identified in the genome sequences of eukaryotes and bacteria and it has been hypothesized that some of them might have been acquired by horizontal gene transfer [41]. SLRs are characterized by a short sequence motif consisting of 36–44 amino acids that fold into pairs of anti-parallel alpha-helices. Full-length SLR proteins comprising 3 to more than 20 repeating units form right-handed super-helical molecules. SLR proteins possess structural similarity with TPR proteins but because of different consensus sequence lengths TPR and SLR proteins differ in their super-helical parameters [25].

The SLR has been named after the *C. elegans* sel-1 gene product (sel: suppressor-enhancer of lin), a molecule that participates in cell-fate control by modulating lin-12 activity [14]. The human homologue Sel1L resides in the endoplasmic reticulum (ER) and translocates misfolded proteins across the ER membrane for degradation in the cytoplasm [5, 20, 32]. Besides the membrane-anchored Sel1L, alternative splicing generates soluble Sel1 isoforms

that have been localized in secretory compartments and in cell/cell contact areas [3]. Differential expression of Sel1L has been associated with increased risks for breast, pancreatic and esophageal cancers [4, 13].

SLR proteins have also been identified in several prokaryotes by genome sequencing experiments but the molecular functions of the vast majority of bacterial SLR proteins are unknown. Functional annotations exist for several SLR proteins from bacteria that live in tight association with eukaryotes, such as *Helicobacter pylori*, *Legionella pneumophila*, *Pseudomonas aeruginosa*, or *Sinorhizobium meliloti* (reviewed in [31]). The SLR proteins LpnE, EnhC, and LidL from *L. pneumophila* enhance the entry of bacteria into host cells [6, 24, 34]. LpnE recognizes several eukaryotic proteins such as obscurin-like protein 1 or the N-terminal domain of the inositol polyphosphate 5-phosphatase OCRL1 [35, 55].

Here, we investigate the molecular function of Helicobacter cystein-rich protein (Hcp) C a SLR protein from the human pathogen *H. pylori*. HcpC belongs to a family of conserved hypothetical proteins, which are characterized by pairs of cysteine residues that cross-link adjacent SLR repeats [29]. All genomes of *H. pylori* strains that have been sequenced so far contain 8 to 9 *hcp* genes. The analysis of several *hcp* genes in a large collection of *H. pylori* strains revealed signatures of positive selection suggesting that some *hcp* gene products are important for the adaptation of *H. pylori* in different human populations [38]. This assumption is corroborated by the observation that some *hcp* genes undergo phase variation to allow *H. pylori* to evade the immune system response [47].

Although most Hcp homologues have been analyzed at the gene level, the detection of high antibody titers against HcpA, -C, and -E confirmed that these molecules are expressed under in vivo conditions and recognized by the human immune system [30]. Serological analysis of *H. pylori* positive patients with different clinical manifestations established HcpC as a virulence factor for chronic atrophic gastritis and gastric cancer sometimes with similar significance scores such as the classical *H. pylori* virulence factors CagA and VacA [12, 15].

Very little is known about the biological functions of Hcp molecules. In cellular assays using murine splenocytes, recombinant HcpA triggered the release of large amounts of the pro-inflammatory cytokines IFN- γ and interleukin-6 [8]. Furthermore, small amounts of HcpA caused morphological changes and enhanced cellular adherence, phagocytosis and CD11b expression in assays using the human myeloid Thp1 cell line [9]. These observations were interpreted as a HcpA-dependent maturation of Thp1 cells from a motile monocytic toward a sessile macrophage-like phenotype.

HcpC did not exert any of these effects. However, the crystal structure of HcpC [26] in conjunction with the cellular functions of HcpA and the results of the serological studies mentioned above gave rise to the hypothesis that HcpC might indeed recognize proteins from the human host. To test this hypothesis, we performed pull-down experiments and validated one putative interaction partner by ELISA and surface plasmon resonance experiments.

Methods

Pull-Down Analysis with Mbp-HcpC

HcpC (hp1098) and HcpA (hp0211) were expressed recombinantly in *E. coli* and purified as described previously [9]. For pull-down experiments, semi-pure Mbp-HcpC with a C-terminal His₆-tag was used. Protein concentrations were determined by UV-spectroscopy using the absorption coefficients ϵ_{280} (Mbp-HcpC) = 1.28 ml cm⁻¹ mg⁻¹, ϵ_{280} (Mbp-HcpA) = 1.27 ml cm⁻¹ mg⁻¹, ϵ_{280} (HcpC) = 0.92 ml cm⁻¹ mg⁻¹ and ϵ_{280} (HcpA) = 0.83 ml cm⁻¹ mg⁻¹.

Pull-down experiments were performed as follows. Thp1 cells were grown up to a density of 10⁶ cells/ml, harvested by centrifugation (200×g, 5 min, 4°C) and washed with ice-cold PBS. Cells were re-suspended in Thp1 lysis buffer (0.2 M sodium chloride, 20 mM Tris-HCl, pH 7.4, 10% glycerol, 0.5% NP-40, 1 tablet Complete protease inhibitor cocktail (Roche) per 50 ml buffer) and kept on ice for 30 min. The lysate was cleared by centrifugation (20,000×g, 45 min, 4°C) and filtration (0.45 μ m filter). Concentration of total protein was adjusted to 10 mg/ml. 60 μ l of amylose affinity resin (New England Biolabs) was washed three times with buffer B (0.2 M sodium chloride, 20 mM Tris, pH 7.4) and split into three aliquots. One aliquot was loaded with Mbp and two aliquots were loaded with Mbp-HcpC. The loaded resin was washed three times with 1 ml buffer B. The Mbp and one Mbp-HcpC loaded aliquots were incubated with a mixture of 500 μ l buffer B and 500 μ l Thp1 cell extract at 4°C overnight with constant agitation. As a negative control, the second Mbp-HcpC loaded aliquot was incubated with 1 ml buffer B. The resin was washed three times with buffer B and the bound proteins were eluted with 30 μ l of 10 mM maltose in buffer B.

After adding 10 μ l SDS-PAGE sample buffer, the samples were analyzed on 12% pre-casted SDS-PAGE gels (BioRad). Gels were stained with colloidal Coomassie Blue (Roth) and each lane was cut into eight gel pieces and transferred into a 96-well plate. Sample preparation was performed with an automated Tecan pipetting station with the following protocol. Samples were destained with 50% acetonitrile (ACN) and reduced with 2 mM TCEP in

25 mM ammonium bicarbonate (ABC) buffer, pH 8.2 for 1 h at 60°C. Free thiol groups were acetylated with 25 mM iodoacetamide in 25 mM ABC buffer for 1 h at darkness. After withdrawal of the supernatant, the gel pieces were washed twice with 50% ACN and digested with 50 ng trypsin per gel piece in ABC buffer at 37°C for 14 h. To terminate the tryptic digestion and to elute peptides, the gel pieces were washed two times with 5% TFA and 50% ACN. After drying the samples in a speed-vac, the peptides were dissolved in 2 M urea, 3% ACN, and 0.1% TFA and desalted using C₁₈ ZipTip® (Millipore) following the instructions of the manufacturer. Re-dissolved samples were injected into an Eksigent-nano-HPLC system (Eksigent Technologies, Dublin, USA) and separated on a self-made reverse-phase tip column (0.075 mm × 80 mm) packed with C₁₈ resin (AQ, 3 µm, 200Å, Bischoff GmbH, Leonberg, Germany). The column was equilibrated with 97% solvent A (1% ACN; 0.2% formic acid in water) and 4% solvent B (80% ACN, 0.2% formic acid in water). Peptides were eluted using the following gradient: 0–5 min, 3–15% B; 5–55 min, 15–50% B; 55–60 min, 50–97% B at a flow rate of 0.2 µl/min. High accuracy mass spectra were acquired at an LTQ-Orbitrap (Thermo Scientific, Bremen, Germany) in the mass range of 300–2,000 *m/z* and a target value of 5×10^5 ions. Up to four data dependent MS/MS were recorded in parallel at the linear ion trap of the most intense ions with charge state 2+ or 3+ using collision-induced dissociation. Target ions already selected for MS/MS were dynamically excluded for 60 s. General mass-spectrometric conditions were: normalized collision energy, 35%; ion selection threshold, 500 counts; activation, 0.25; and activation time, 30 ms for MS/MS acquisitions. Peak lists were generated using Mascot Distiller software 2.1.1 (Matrix Science Ltd., London, UK) and searched against the protein database from UniProt_20100127 (www.uniprot.org) using the Mascot search algorithm (Mascot 2.3). Peptide and protein assignments were filtered for peptide probabilities greater than 95% and protein probabilities greater than 99%. Identified proteins must contain at least two peptides. The list was manually curated for false-positive hits (e.g. glycogen phosphorylase). These false-positive hits were not automatically recognized in the control experiments, because peptides were assigned to a different database entry.

Expression and Purification of Nek9

Expression of Nek9 in Hek293 cells was described previously [45]. Briefly, the expression plasmid pCMV5flag-Nek9 was a kind gift from Prof. Joe Avruch (Harvard Medical School, Boston). Four 15 cm culture dishes were inoculated with 1 ml Hek293 cells each. Cells were grown

in 25 ml DMEM-GlutaMAX™ medium (Gibco) supplemented with 10% fetal calf serum and 1% PenStrep (100 U/ml final concentration, Gibco) at 37°C and 5% carbon dioxide. When cells reached 50% confluence they were transfected with 0.4 µg pCMV5flag-Nek9 vector per milliliter medium using the polyethylenimine (linear polyethylenimine, Mw 25000, Polyscience Inc.) transfection method [10]. After 24 h the medium was withdrawn, cells were washed with ice-cold PBS and detached with 10 mM EDTA in ice-cold PBS. Cells were harvested by centrifugation (200×*g*, 4 min, 4°C) and lysed in 10 ml Hek lysis buffer (0.15 M sodium chloride, 50 mM Tris-HCl, pH 7.1, 1 mM DTT, 1 mM EDTA, 0.6 mM EGTA, 1% (v/v) Triton X-100, 1 mM sodium vanadate, 1 tablet Complete-EDTA free protease inhibitor cocktail (Roche) per 50 ml lysis buffer) for 20 min under constant agitation at 4°C.

The lysate was cleared by centrifugation (5,000×*g*, 20 min, 4°C). The extract was either directly used for crude-cell extract ELISA or loaded onto a 0.4 ml anti-flag antibody affinity column (Sigma), which was equilibrated with TBS (140 mM sodium chloride, 10 mM Tris-HCl, pH 7.4). The column was washed with 10 column volumes (CV) TBS until no protein eluted from the column. Purified Nek9 was eluted by 5 CV 3-flag peptide (Sigma) in TBS at a concentration of 0.1 mg/ml. Protein containing fractions were pooled and the buffer was replaced against TBS supplemented with 10% (v/v) glycerol by ultrafiltration. Aliquots of Nek9 at a concentration of 0.2 mg/ml were stored at –80°C. Protein concentration was determined by UV-spectroscopy (ϵ_{280} (Nek9) = 0.99 ml cm⁻¹ mg⁻¹) using the flow-through of the concentration step as a blank. Protein purity was investigated using silver stained 12% Laemmli gels or western-blot analysis. Gels were blotted onto nitrocellulose membranes and analyzed using a primary anti-flag mouse antibody (Sigma, 1:2000 dilution) and an anti-mouse IgG secondary antibody conjugated to horseradish peroxidase (Sigma, 1:4000 dilution). Blots were stained using a luminescence kit (GE Healthcare) according to the guidelines of the manufacturer.

Binding Analysis by ELISA

All ELISA experiments were performed in Nunc Maxisorb 96-well plates. All volumes were 50 µl/well if not stated differently. After every step, the plate was washed three times with water and three times with TBST (0.14 M sodium chloride, 10 mM Tris-HCl, 0.2% (v/v) Tween-20, pH 7.4). All binding steps were performed in B-TBST (0.5% (w/v) BSA in TBST). For dose-response curves, HcpA and HcpC were diluted in TBS to final concentrations of 0.01 µg/µl and each well was coated for 90 min at room temperature under constant agitation. To avoid

unspecific binding, wells were blocked with 200 μl 2% (w/v) BSA in TBST at 4°C over night.

Serial dilutions of Hek293 cell extracts expressing flag-tagged Nek9 in B-TBST were added and the plate was incubated for 1 h at 4°C. Initial protein concentration of cell extract was measured by Bradford analysis (BioRad) using BSA as a standard. Bound Nek9 was detected by an anti-flag mouse antibody (Sigma, 1:3000 dilution) and the bound primary antibody was detected by an anti-mouse IgG antibody conjugate to horseradish peroxidase (Sigma, 1:5000 dilution) unless stated differently. Both antibodies were incubated for 1 h at room temperature. Finally, 100 μl 3,3',5,5'-tetramethylbenzidine reagent (Sigma) was added for 3 to 4 min. The reaction was stopped with 2 M sulfuric acid and the absorption was measured at 450 nm in an ELISA-plate reader (Tecan).

For competition ELISA experiments, 10 nM Nek9 was pre-incubated with HcpC at different concentrations for 1 h at room temperature. Binding of Nek9/HcpC mixtures to immobilized HcpC (0.15 $\mu\text{g}/\text{well}$) was reduced to 10 min at room temperature and the amount of bound Nek9 was determined as described before. Data were analyzed using program SigmaPlot Version 11 (Systat Software). To obtain the dissociation constant from the crude-cell extract competition ELISA, the inverse of the fractional saturation ($1/v$) was plotted over the inverse of the total HcpC concentration ($1/a0$) as described in [11]. Competition ELISA data using purified proteins were analyzed by Scatchard analysis and by nonlinear curve fitting. Data were fitted to the single hyperbolic function $v = (v_{\text{max}} \times a0)/(K_d + a0)$. For Scatchard analysis, v/a was plotted over the fractional saturation of Nek9 (v), which corresponds to $(A0 - A)/A0$. A refers to the background subtracted absorptions at 450 nm at a given HcpC concentration. $A0$ refers to the absorption in the absence of HcpC. The concentration of free HcpC (a) corresponds to $a0 - i0 \times v$ with $a0$ being the total concentration of HcpC and $i0$ the total concentration of Nek9 [11].

Surface Plasmon Resonance

SPR interaction analyses were performed using a Biacore T100 optical biosensor (Biacore Life Sciences/GE Healthcare, Uppsala, Sweden). Series S Sensor Chips CM5, *N*-hydroxysuccinimide (NHS), *N*-ethyl-*N'*-(3-dimethylaminopropyl)carbodiimide (EDC), and ethanolamine-HCl, as well as sampling vials, and caps, were obtained from Biacore. Data were collected with the biosensor instrument at 20°C. A solution of 10 mM HEPES, 0.15 M NaCl, 3 mM EDTA, and 0.05% (v/v) surfactant P20, pH 7.4 was used as running buffer.

To prepare the sensor chip for interaction analysis, a series of solutions were injected over the chip surface. A

new CM5 sensor chip was inserted into the instrument and the instrument primed with running buffer. The conditioning solutions (100 mM HCl, 50 mM NaOH, 0.5% (w/v) SDS, and water) were used to hydrate and clean the dextran layer. Two aliquots of each conditioning solution were injected over all four flow cells (Fc) for 60 s at a flow rate of 100 $\mu\text{l}/\text{min}$.

A solution of 10 mM sodium acetate, pH 5.0 was used as immobilization buffer. To minimize denaturation, Nek9 was diluted into the immobilization buffer only immediately before use to a final concentration of 40 $\mu\text{g}/\text{ml}$. Using a flow rate of 10 $\mu\text{l}/\text{min}$, the surface of Fc2 was activated for 7 min using a 1:1 mixture of 0.1 M NHS and 0.4 M EDC, and 40 $\mu\text{g}/\text{ml}$ Nek9 in immobilization buffer was injected until 2500 RU were immobilized. This was followed by the injection of a 0.1 mg/ml solution of BSA in 10 mM sodium acetate, pH 5.0 until a final total surface density of 6,000 RU was reached. Residual-activated groups on the surface were blocked by a 7 min injection of 1 M ethanolamine-HCl, pH 8.5. The reference flow cell was coated as described for the flow cell with 6,000 RU BSA only. An initial series of buffer blanks was injected first to fully equilibrate the system. The analyte (HcpC) samples were analyzed first from the lowest to the highest concentration and then run in duplicate from the highest to the lowest concentration. During each binding cycle, the analyte was injected for 4 min at a flow rate of 50 $\mu\text{l}/\text{min}$ and dissociation was monitored for 900 s. The storage buffer of the HcpC stock solution was replaced by the running buffer by ultrafiltration. To completely remove remaining amounts of HcpC bound to the sensor chip surface, regenerations were performed by single 30 s injections of 10 mM Na_2CO_3 , 0.3 M KCl, pH 10 at a flow rate of 30 $\mu\text{l}/\text{min}$.

Data collected on an SPR biosensor require processing to remove systematic artifacts coming from nonspecific binding, signal drift, and bulk refractive index changes. Data sets were processed and analyzed using Biacore T100 Evaluation Software. Double referenced data for HcpC were globally fitted to a simple 1:1 interaction steady-state affinity model [33].

Results

Identification of HcpC Interaction Partners by Pull-Down Proteomics

To identify putative interaction partners, we expressed HcpC with a N-terminal Mbp- and a C-terminal His₆-tag [9]. After the first purification step, the semi-pure Mbp-HcpC fusion protein was bound to amylose beads and the immobilized fusion protein was incubated with Thp1 cell

Table 1 Proteins that were identified from Thp1 cell extracts by pull-down with Mbp-HcpC

Protein	Uniprot ID	Unique peptides	Peptides identified	Sequence coverage (%)	Mascot protein score
Heat shock protein HSP 90-beta	Q9NTK6	7	ADLNNLGTIAK GVVDSDELPLNISR HLEINPDHPVETLR NPDDITQEEYGEFYK TLTLVDTGIGMTK VILHLKEDQTEYLEER YHTSQSGDEMTSLSEYVSR	14	267
Serine/threonine-protein kinase Nek9	Q8TD19	6	GAFGEATLYR KLEGGQQVGMHSK LGINLLGGPLGGK LGLDSEEDYYTPQKVDVPK STPQKLDVIK VASEAPLEHKPQVEASSPR	9	197
Tubulin alpha-ubiquitous chain	P68363	4	AVFVDLEPTVIDEVR QLFHPEQLITGKEDAANNYAR TIGGGDDSFNTFFSETGAGK VGINYQPPTVVPGGDLAK	16	183
Heat shock cognate 71 kDa protein	P11142	4	LSKEDIER NSLESYAFNMK TTPSYVAFTDTER VQVEYKGETK	6	180
Malectin	Q14165	2	KFAEVYFAQSQQKV RSNPEDQILYQTERY	8	155
Heterogeneous nuclear ribonucleoprotein U	Q00839	2	NFIELDQTNVSAQAQR QMADTGKLNLTLLQR	3	116
Transcription factor ETV6	P41212	5	ALLLLTKEDFR LSEDGLHR SPLDNMIR TNMITYEK TPDEIMSGR	9	113
Nucleolin	P19338	4	ATFIKVPQNQNGK GFGFVDFNSEEDAK GLSEDTEETLKESFDGSVR IVTDRETGSSK	8	92

extract. Putative HcpC interaction partners co-eluted under mild conditions using 10 mM maltose and were identified using established procedures. To reject proteins that either recognized the Mbp-tag or that were unspecific absorbed to the amylose matrix control experiments with immobilized Mbp were performed. Control experiments with immobilized Mbp-HcpC in the absence of cell extract allowed the rejection of contaminations from the Mbp-HcpC purification.

Proteins that co-eluted with Mbp-HcpC but were absent from the negative control experiments are summarized in Table 1. One of the most significant putative interaction partners is the NimA-like protein kinase Nek9,

which is involved in the control of spindle dynamics and chromosome separation [45]. Nek9 is a cytoplasmic protein that comprises a N-terminal protein kinase domain and a central domain that contains seven regulator of chromosome condensation 1 (RCC1) repeats. The six identified peptides were equally distributed over the entire sequence, indicating that full-length Nek9 was identified. The remaining hits can be clustered into three groups: (i) molecular chaperones, (ii) nucleic acid binding proteins, and (iii) miscellaneous hits.

(i) Several heat shock proteins (Hsp) co-eluted with Mbp-HcpC. Besides the heat shock cognate (Hsc) 71 protein, we identified the beta-isoform of Hsp90. Hsp90 is

regarded as a ubiquitous cytoplasmic protein that participates in protein folding, transportation, degradation, and cell signalling events (reviewed in [40]). Hsc71 is a constitutively expressed molecular chaperone located in the cytoplasm and at the cell surface [49], which also participates in membrane trafficking (reviewed in [22]) and antigen maturation [21].

(ii) Three proteins were identified that recognize nucleic acids. Nucleolin and transcription factor ETV6 are both localized in the nucleus and the cytoplasm. In the nucleus, nucleolin recognizes pre-mRNA splice sites and telomeric DNA sequences [17]. However, nucleolin was also localized at the plasma membrane surface [50]. The heterogeneous nuclear ribonucleoprotein U (hnRNP U) also recognizes single- and double-stranded DNA and mRNA. It is regarded as a nuclear and cytoplasmic protein, where it participates in the spliceosome C complex. However, together with nucleolin it has previously been localized at the plasma membrane [19]. The transcription factor ETV6 can inhibit Ras-dependent growth and comprises two domains, a N-terminal SAM-like protein recognition domain and a C-terminal ETS-like DNA-binding domain [57].

(iii) The last cluster contains the ubiquitous tubulin- α chain. Tubulin- α and tubulin- β form dimers that build up the microtubule protofilament. Tubulin- β was also recognized in the Mbp-HcpC pull-down experiments. Since it was present in the negative control tubulin- β is not listed in Table 1. Malectin is anchored in the ER membrane where it might be involved in the processing and secretion of *N*-glycosylated proteins [48].

Validation of the Interaction Between Nek9 and HcpC by Crude-Cell Extract ELISA

Since the validation of all eight putative HcpC interaction partners was beyond the scope of this study, we selected one possible hit for further in vitro analysis. We unselected Hsp90 and tubulin because these hits are highly expressed in Thp1 cells. We rather concentrated on Nek9, because this hit was clearly identified in the pull-down experiment albeit its weak expression in Thp1 cells and further evidence came from a sequence database search. According to the Rosetta stone model, certain domains are predicted to interact because their homologues are fused in a so called Rosetta stone protein [27]. Thus, a Rosetta stone protein that would support an interaction between Nek9 and HcpC would contain a SLR domain fused to either a protein kinase domain or a RCC1 domain. Domain architectures with N-terminal protein kinase and C-terminal SLR domains are for example predicted for the *Thermobifida fusca* Tfu_1658 gene product (Uniprot ID: Q47PC6), the *Naegleria gruberi* 67437 gene product (Uniprot ID:

D2VEY2), or human eukaryotic elongation factor 2 kinase (Uniprot ID: O00418).

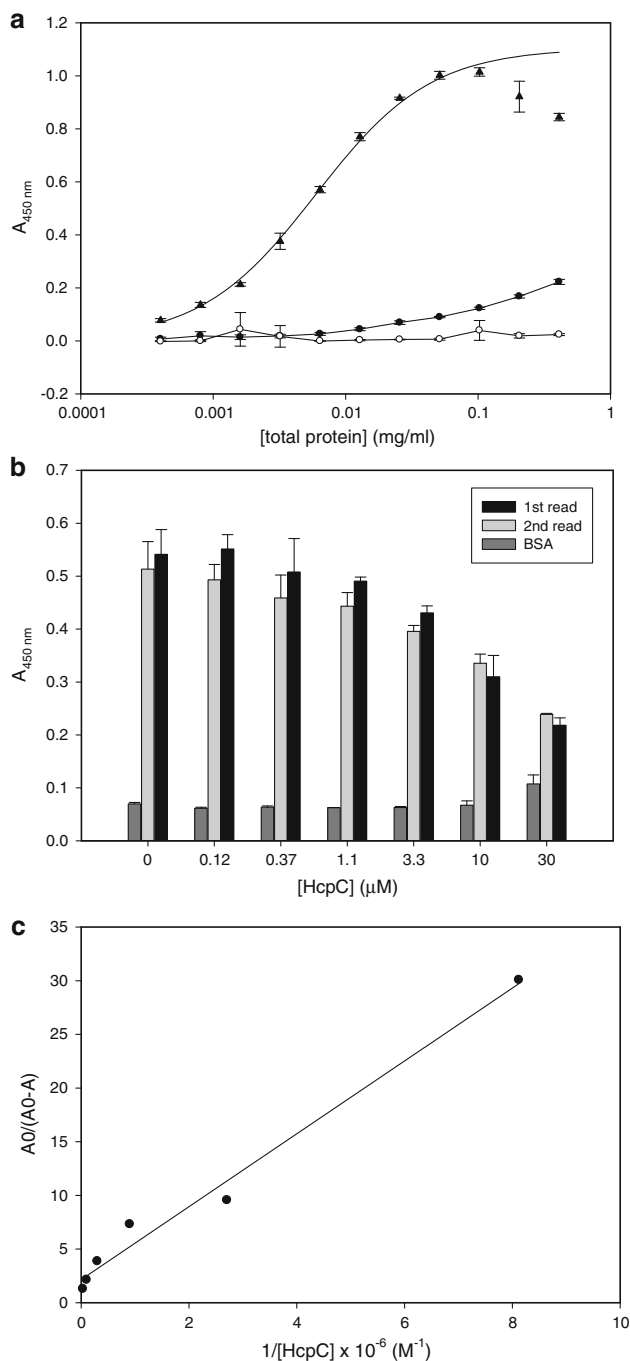
To validate this interaction, flag-tagged Nek9 was expressed in Hek293 cells as described previously [45]. HcpC and its close homologue HcpA were immobilized in 96-well plates and incubated with different amounts of Nek9-expressing Hek293 cell extracts. The amounts of bound Nek9 were quantified using an anti-flag antibody. The dose-response curve reveals a clear interaction between soluble Nek9 and immobilized HcpC, whereas no such interaction was detected between Nek9 and HcpA despite the high level of sequence identity among Hcps (Fig. 1a). At protein concentrations above 100 $\mu\text{g/ml}$, the amount of HcpC-bound Nek9 decreases, which can be explained by a reduction of the affinity of Nek9 for HcpC because of the high concentration of Triton X-100 in cell extracts. Similar results have been obtained with the uncleaved Mbp-HcpC and Mbp-HcpA fusion proteins confirming that the N-terminal Mbp-tag does not prevent the interaction between Nek9 and HcpC (data not shown).

To eliminate the possibility that Nek9 recognizes epitopes that become exposed upon immobilization of HcpC and to obtain a quantitative estimate for the Nek9/HcpC binding affinity the interaction was investigated using a competition ELISA set-up. Here, the concentration of free Nek9 in mixtures between crude-cell extracts and HcpC at different concentrations was measured by ELISA. To confirm that the interaction between Nek9 and immobilized HcpC does not shift the equilibrium between Nek9 and soluble HcpC, the Nek9/HcpC mixtures were analyzed by two subsequent ELISA experiments. Since the signal of the first measurement deviates less than 12% from the second measurement the data were investigated by Scatchard analysis and revealed a dissociation constant (K_d) of $(3.4 \pm 0.2) \mu\text{M}$ (Fig. 1b, c).

Nek9 Recognizes HcpC with High Affinity

To investigate the possibility that the interaction between Nek9 and HcpC is mediated by an endogenous protein, Nek9 was purified from Hek293 cells by affinity chromatography and the interaction was investigated by competition ELISA and surface plasmon resonance analysis. Nek9 was purified at a yield of 21 μg from a 100 ml Hek293 cell culture. SDS-PAGE analysis revealed one major band that represents Nek9, because it occurs at the expected molecular weight and it is recognized by an anti-flag antibody. However, the analysis also revealed a contamination with a molecular weight of approximately 70 kDa that was shown to be Hsc71 by in-gel proteolytic digestion and mass-spectrometric analysis of peptides (Fig. 2a).

In a first approach, HcpC was immobilized in 96-well plates and the interaction between immobilized HcpC and



semi-pure Nek9 was inhibited by varying the concentrations of soluble HcpC at a constant concentration of Nek9. The dissociation constant between HcpC and purified Nek9 was determined by directly fitting the fractional saturation as a function of total HcpC added (Fig. 2b). This analysis revealed a dissociation constant of $(0.5 \pm 0.2) \mu\text{M}$. The Scatchard plot shows a straight line that intersects the x-axis at 0.9, suggesting a 1:1 stoichiometry between Nek9 and HcpC. Since the concentration of semi-pure Nek9 (10 nM) is much smaller than the dissociation constant, this analysis provides only a rough estimate [56].

Fig. 1 a Crude-cell extract ELISA of immobilized HcpC (black triangles), HcpA (black spheres), and BSA (open spheres) with crude extract of Hek293 cells expressing flag-tagged Nek9. Error bars represent standard deviations of individual measurements (three measurements for HcpA and HcpC, two measurements for BSA). The HcpC/Nek9 interaction data excluding the two measurements at highest protein concentrations were fitted by a hyperbolic function ($R = 0.9990$). **b** Competition ELISA using extracts of Nek9 expressing Hek293 cells. The absorbance at 450 nm is plotted over the concentration of soluble HcpC using a constant amount of cell extract (0.05 mg/ml total protein concentration). The HcpC/cell extract mixtures were incubated in wells with 0.15 $\mu\text{g}/\text{well}$ immobilized HcpC (1st read). After 10 min, the mixture was transferred to a second well and incubated for the same time (2nd read). The background was estimated by incubating the mixture in wells where BSA was immobilized instead of HcpC (BSA). Error bars represent standard deviations for three and two measurements for HcpC- and BSA coated wells, respectively. **c** Scatchard analysis of crude-cell extract competition ELISA. Data were fitted to a linear equation ($R = 0.9920$) revealing a dissociation constant of K_d equals $(3.4 \pm 0.2) \mu\text{M}$

In a second approach, the binding of soluble HcpC to Nek9 was investigated by surface plasmon resonance (SPR) analysis. In contrast to the ELISA experiments where soluble Nek9 interacted with immobilized HcpC the set-up was inverted. In the SPR set-up, Nek9 was immobilized on the chip surface and the interaction with soluble HcpC at concentrations between 90 and 7,290 nM was monitored. Since association and dissociation rates were extremely fast, reliable k_{on} and k_{off} values could not be determined. Instead K_d was calculated based on steady-state kinetics (Fig. 2c). The equilibrium dissociation constant as determined from steady-state affinity fitting was 28 μM . SPR analysis also confirmed that immobilized Nek9 is not recognized by soluble HcpA (inset in Fig. 2c).

Discussion

The implication of eukaryotic SLR proteins in cell-fate control and the reported interactions between bacterial SLR proteins and host cells [6, 9, 24, 34] prompted us to identify human proteins that could interact with HcpC from *H. pylori*. Using HcpC that was immobilized by its N-terminal Mbp-tag and extracts from human Thp1 cells, we identified eight putative interaction partners with reasonable significance.

Interestingly, several putative interaction partners are localized in the cytoplasm or the nucleus. Only malectin, Hsc71, hnRNP U, and nucleolin were reported to be expressed either in the ER-lumen or at the cellular surface. Although nucleolin is considered to be a nuclear or cytoplasmic protein it serves as a receptor for bacterial adherence. Nucleolin that was localized at the plasma membrane recognized the bacterial adherins intimin-alpha, -beta and -gamma with high affinity [50, 51]. Therefore, nucleolin

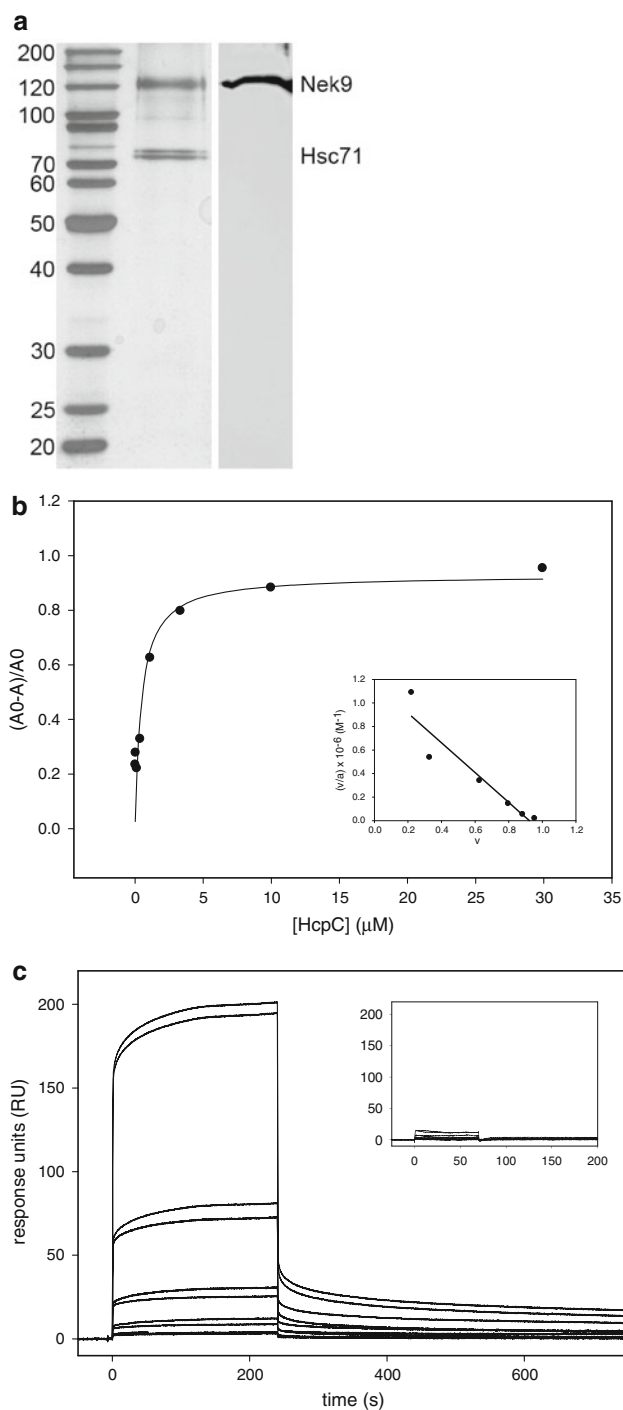


Fig. 2 a Western-blot analysis of Hek293 cell extract expressing Nek9 using an anti-flag mouse antibody (*right side*) and silver stained gel of affinity purified Nek9 (*left side*). The analysis revealed one major contamination that co-eluted with Nek9. This contamination was shown to be Hsc71 by in-gel digestion with trypsin followed by LC-MS/MS analysis and the assignment of eight unique peptides. **b** Competition ELISA between flag-tagged Nek9 and HcpC at different concentrations. Nek9 bound to immobilized HcpC was quantified using an anti-flag mouse antibody. Fractional saturation was plotted over the concentration of soluble HcpC. Data were fitted as a single hyperbolic function ($R = 0.9269$) as described in “Methods” section and reveals a K_d of $(0.5 \pm 0.2) \mu\text{M}$. The *inset* shows the Scatchard analysis of the data. **c** Surface plasmon resonance sensograms for the interaction between HcpC and Nek9. Nek9 was covalently bound to the biosensor surface. Each HcpC concentration (90, 270, 810, 2430, and 7290 nM) was injected twice. The *inset* shows the sensograms for the interaction between HcpA and Nek9. Each HcpA concentration (402, 804, 1608, 3216, and 6432 nM) was injected twice. Fitting of double referenced data to a steady-state affinity model gives a K_d of 165 nM for the HcpA/Nek9 interaction

functions human Hsc71 serves as a receptor for the uptake of *Listeria monocytogenes* and *Brucella abortus* into trophoblast giant cells. This process is mediated by the binding of bacterial TPR proteins to the C-terminal EEVD motif from Hsc71 [52]. HcpC can be regarded as a bacterial TPR protein, because it was shown that the crystal structures of HcpC and heat shock organizing protein (Hop), which also belongs to the family of TPR proteins, are very similar [26]. Furthermore, the conformations and receptor/peptide interactions are almost identical in HcpC, which recognizes its own C-terminus, and Hop, which binds to the C-terminus of Hsp70 and thereby serves as an adaptor protein that links Hsp70 to Hsp90 (reviewed in [37]). Hsc71 and Hsp70 share 86% sequence identity and Hsc71 interacts with Hop in as similar manner like Hsp70 [7]. From a pure structural point of view HcpC could serve as a bacterial adaptor that links Hsc71 and Hsp90 in a similar manner like Hop.

Furthermore, the co-chaperones Hsc71 and Hsp70 regulate the immune response of antigen presenting cells by modulating the transient aggregation of proteins [21]. Interfering with this process is an efficient strategy for pathogens such as *L. pneumophila* to readjust the immune response of the host, because the aggregation of proteins ultimately guides the maturation of dendritic cells [18, 23]. Since recombinant HcpA fosters the maturation of Thp1 cells from a monocytic toward a macrophage-like phenotype [9] the analysis of the interactions between HcpA, HcpC, Hsp70, Hsc71, and Hsp90 merits further investigation.

In this report, we concentrated on the interaction between HcpC and Nek9, because Nek9 was one of the most significant hits in the pull-down analysis. The hypothesis that HcpC and Nek9 could interact was further supported by the identification of proteins with fused

would be in the proper position to recognize secreted or membrane-associated HcpC. Surface-exposed nucleolin serves as a receptor for other *H. pylori* proteins, such as the TNF-alpha inducing protein and this interaction has been implicated in the carcinogenesis of *H. pylori* [53, 54].

Two very promising hits are Hsc71 and Hsp90, since both proteins are associated with various processes that lead to the uptake of bacteria or the signaling that follows bacterial infection (reviewed in [42]). Among other

protein kinase and SLR domains. The Rosetta stone model predicts that domains that participate in a protein complex can reside either on a single polypeptide chain or on separate chains in different species [27]. The crude-cell extract ELISA confirms the initial hypothesis and reveals that the interaction between HcpC and Nek9 is very specific, because immobilized HcpA was not recognized by Nek9, although HcpA and HcpC share 56% sequence identity (Fig. 1a). This result is consistent with the SPR analysis where also no interaction between HcpA and Nek9 could be observed (inset in Fig. 2c).

To obtain an estimate for the binding affinity, the interaction between purified Nek9 and HcpC was investigated using three different experimental set-ups. All methods consistently yielded dissociation constants in the lower micromolar range between 0.5 and 28 μM . The broad spread could be a consequence of different experimental set-ups and methods to process the data. In the competition ELISA experiments, K_d values were determined by using immobilized HcpC and soluble Nek9, whereas for the SPR analysis immobilized Nek9 and soluble HcpC were used. To show that HcpC directly interacts with Nek9, experiments with purified proteins were performed. However, over-expressed Nek9 was always contaminated with Hsc71 and all attempts to remove this contamination were so far unsuccessful. Interestingly, already the pull-down experiments suggested that Hsc71 could interact with HcpC. Therefore, we cannot discern if HcpC binds either directly to Nek9 or to a Nek9/Hsc71 complex.

Nek9, which is also called Nercc1, belongs to the family of NimA-like protein kinases that are characterized by a well conserved N-terminal protein kinase domain and different C-terminal domains (reviewed in [36]). In Nek9, seven RCC1 repeats occupy the position of the C-terminal domain. Nek9 plays an important role in microtubule organization [16, 45] and modulates the activities of further NimA-like protein kinases, such as Nek6 and Nek7 [1]. Studies using the *Xenopus* homologue showed that Nek9 is associated with the gamma-tubulin ring complex [44].

The biological significance of the HcpC/Nek9 interaction is currently unclear and the implications of Nek9 during pathogen infections are just emerging. A recent proteomics study revealed that upon infection with *L. monocytogenes* the phosphorylation states of various protein kinases are modified. Residue Thr333 of Nek9 becomes phosphorylated after treatment with internalin B, an important stimulant for the uptake of *L. monocytogenes* into host cells [43]. This site is located in close proximity to an established nuclear localization signal of Nek9. In a second study, it was shown that the sub-cellular distribution of Nek9 was modified in response to binding of the human adenovirus E1A protein to Nek9. It was suggested

that E1A—one of the first proteins that are transcribed after adenoviral infection—alters the function of Nek9 in the nucleus [39]. These results show that Nek9 is indeed targeted by various factors upon the invasion of bacteria or viruses.

The interaction between TPR proteins, which are structurally similar to SLR proteins like HcpC, and protein kinases are well established. One of the best studied examples is the interaction between P58^{IPK} and RNA-activated protein kinase (PKR). P58^{IPK} consists of 9 TPRs and a C-terminal DnaJ-like domain and participates in the unfolded protein response during ER-stress conditions. The PKR binding site was mapped to TPR No. 6 of P58^{IPK}, whereas the binding site for Hsp40 is located in the DnaJ-like domain (reviewed in [28]).

Besides the implication of Nek9 in *H. pylori* infection, the present study raises a few additional questions, like for example how HcpC and Nek9 get in touch. HcpC is an extremely stable molecule with a melting temperature of 65°C, which is either secreted into the culture supernatant or absorbed to the outer membrane of *H. pylori* cells [2, 26, 46]. The HcpC homologues LpnE, EnhC, and LidL are known to confer phagocytotic uptake of *L. pneumophila* into host cells [6, 24, 34] and the *H. pylori* homologue HcpA reveals a similar activity (P.R.E.M. unpublished observation). Therefore, HcpC would be in the proper position to enter the phagosome but these experiments do not answer the question how HcpC penetrates from the phagosome into the cytoplasm. Perhaps, its extraordinary stability enables HcpC to survive the final stages of the phagolysosome. Further studies are clearly necessary to resolve these questions.

Acknowledgment This work was supported by a grant from the Velux Foundation (Zürich, Switzerland) to P.R.E.M. and Prof. J. Fritz-Steuber.

References

1. Belham C, Roig J, Caldwell JA et al (2003) A mitotic cascade of NIMA family kinases. Nercc1/Nek9 activates the Nek6 and Nek7 kinases. *J Biol Chem* 278:34897–34909
2. Bumann D, Aksu S, Wendland M et al (2002) Proteome analysis of secreted proteins of the gastric pathogen *Helicobacter pylori*. *Infect Immun* 70:3396–3403
3. Cattaneo M, Lotti LV, Martino S et al (2009) Functional characterization of two secreted SEL1L isoforms capable of exporting unassembled substrate. *J Biol Chem* 284:11405–11415
4. Cattaneo M, Orlandini S, Beghelli S et al (2003) SEL1L expression in pancreatic adenocarcinoma parallels SMAD4 expression and delays tumor growth in vitro and in vivo. *Oncogene* 22:6359–6368
5. Christianson JC, Shaler TA, Tyler RE et al (2008) OS-9 and GRP94 deliver mutant alpha1-antitrypsin to the Hrd1-SEL1L ubiquitin ligase complex for ERAD. *Nat Cell Biol* 10:272–282

6. Cirillo SL, Lum J, Cirillo JD (2000) Identification of novel loci involved in entry by *Legionella pneumophila*. *Microbiology* 146: 1345–1359
7. Demand J, Luders J, Hohfeld J (1998) The carboxy-terminal domain of Hsc70 provides binding sites for a distinct set of chaperone cofactors. *Mol Cell Biol* 18:2023–2028
8. Deml L, Aigner M, Decker J et al (2005) Characterization of the *Helicobacter pylori* cysteine-rich protein A as a T-helper cell type 1 polarizing agent. *Infect Immun* 73:4732–4742
9. Dumrese C, Slomianka L, Ziegler U et al (2009) The secreted *Helicobacter* cysteine-rich protein A causes adherence of human monocytes and differentiation into a macrophage-like phenotype. *FEBS Lett* 583:1637–1643
10. Ehrhardt C, Schmolke M, Matzke A et al (2006) Polyethylenimine, a cost-effective transfection reagent. *Signal Transduction* 6: 179–184
11. Friguet B, Chaffotte AF, Djavadi-Ohanian L et al (1985) Measurements of the true affinity constant in solution of antigen-antibody complexes by enzyme-linked immunosorbent assay. *J Immunol Methods* 77:305–319
12. Gao L, Weck MN, Michel A et al (2009) Association between chronic atrophic gastritis and serum antibodies to 15 *Helicobacter pylori* proteins measured by multiplex serology. *Cancer Res* 69: 2973–2980
13. Granelli P, Cattaneo M, Ferrero S et al (2004) SEL1L and squamous cell carcinoma of the esophagus. *Clin Cancer Res* 10: 5857–5861
14. Grant B, Greenwald I (1996) The *Caenorhabditis elegans* sel-1 gene, a negative regulator of lin-12 and glp-1, encodes a predicted extracellular protein. *Genetics* 143:237–247
15. Haas G, Karaali G, Ebermayer K et al (2002) Immunoproteomics of *Helicobacter pylori* infection and relation to gastric disease. *Proteomics* 2:313–324
16. Holland PM, Milne A, Garka K et al (2002) Purification, cloning, and characterization of Nek8, a novel NIMA-related kinase, and its candidate substrate Bicd2. *J Biol Chem* 277:16229–16240
17. Ishikawa F, Matunis MJ, Dreyfuss G et al (1993) Nuclear proteins that bind the pre-mRNA 3' splice site sequence r(UUAG/G) and the human telomeric DNA sequence d(TTAGGG)n. *Mol Cell Biol* 13:4301–4310
18. Ivanov SS, Roy CR (2009) Modulation of ubiquitin dynamics and suppression of DALIS formation by the *Legionella pneumophila* Dot/Icm system. *Cell Microbiol* 11:261–278
19. Jordan P, Heid H, Kinzel V et al (1994) Major cell surface-located protein substrates of an ecto-protein kinase are homologs of known nuclear proteins. *Biochemistry* 33:14696–14706
20. Kaneko M, Yasui S, Niinuma Y et al (2007) A different pathway in the endoplasmic reticulum stress-induced expression of human HRD1 and SEL1 genes. *FEBS Lett* 581:5355–5360
21. Ketter N, Rogon C, Limmer A et al (2011) The Hsc/Hsp70 co-chaperone network controls antigen aggregation and presentation during maturation of professional antigen presenting cells. *PLoS One* 6:e16398
22. Kirchhausen T (2000) Three ways to make a vesicle. *Nat Rev Mol Cell Biol* 1:187–198
23. Lelouard H, Gatti E, Cappello F et al (2002) Transient aggregation of ubiquitinated proteins during dendritic cell maturation. *Nature* 417:177–182
24. Liu M, Conover GM, Isberg RR (2008) *Legionella pneumophila* EnhC is required for efficient replication in tumour necrosis factor alpha-stimulated macrophages. *Cell Microbiol* 10:1906–1923
25. Lüthy L, Grütter MG, Mittl PR (2002) The crystal structure of *Helicobacter pylori* cysteine-rich protein B reveals a novel fold for a penicillin-binding protein. *J Biol Chem* 277:10187–10193
26. Lüthy L, Grütter MG, Mittl PR (2004) The crystal structure of *Helicobacter* cysteine-rich protein C at 2.0 Å resolution: similar peptide-binding sites in TPR and SEL1-like repeat proteins. *J Mol Biol* 340:829–841
27. Marcotte EM, Pellegrini M, Ng HL et al (1999) Detecting protein function and protein-protein interactions from genome sequences. *Science* 285:751–753
28. Melville MW, Katze MG, Tan SL (2000) P58IPK, a novel co-chaperone containing tetratricopeptide repeats and a J-domain with oncogenic potential. *Cell Mol Life Sci* 57:311–322
29. Mittl PR, Lüthy L, Hunziker P et al (2000) The cysteine-rich protein A from *Helicobacter pylori* is a beta-lactamase. *J Biol Chem* 275:17693–17699
30. Mittl PR, Lüthy L, Reinhardt C et al (2003) Detection of high titers of antibody against *Helicobacter* cysteine-rich proteins A, B, C, and E in *Helicobacter pylori*-infected individuals. *Clin Diagn Lab Immunol* 10:542–545
31. Mittl PR, Schneider-Brachert W (2007) Sel1-like repeat proteins in signal transduction. *Cell Signal* 19:20–31
32. Mueller B, Lilley BN, Ploegh HL (2006) SEL1L, the homologue of yeast Hrd3p, is involved in protein dislocation from the mammalian ER. *J Cell Biol* 175:261–270
33. Myszkka DG (1999) Improving biosensor analysis. *J Mol Recognit* 12:279–284
34. Newton HJ, Sansom FM, Bennett-Wood V et al (2006) Identification of *Legionella pneumophila*-specific genes by genomic subtractive hybridization with *Legionella micdadei* and identification of lpnE, a gene required for efficient host cell entry. *Infect Immun* 74:1683–1691
35. Newton HJ, Sansom FM, Dao J et al (2007) Sel1 repeat protein LpnE is a *Legionella pneumophila* virulence determinant that influences vacuolar trafficking. *Infect Immun* 75:5575–5585
36. O'Regan L, Blot J, Fry AM (2007) Mitotic regulation by NIMA-related kinases. *Cell Div* 2:25
37. Odunuga OO, Longshaw VM, Blatch GL (2004) Hop: more than an Hsp70/Hsp90 adaptor protein. *Bioessays* 26:1058–1068
38. Ogura M, Perez JC, Mittl PR et al (2007) *Helicobacter pylori* evolution: lineage-specific adaptations in homologs of eukaryotic Sel1-like genes. *PLoS Comput Biol* 3:e151
39. Pelka P, Scime A, Mandalfino C et al (2007) Adenovirus E1A proteins direct subcellular redistribution of Nek9, a NIMA-related kinase. *J Cell Physiol* 212:13–25
40. Picard D (2002) Heat-shock protein 90, a chaperone for folding and regulation. *Cell Mol Life Sci* 59:1640–1648
41. Ponting CP, Aravind L, Schultz J et al (1999) Eukaryotic signalling domain homologues in archaea and bacteria. Ancient ancestry and horizontal gene transfer. *J Mol Biol* 289:729–745
42. Pratt WB, Morishima Y, Peng HM et al (2010) Proposal for a role of the Hsp90/Hsp70-based chaperone machinery in making triage decisions when proteins undergo oxidative and toxic damage. *Exp Biol Med (Maywood)* 235:278–289
43. Reinl T, Nimtz M, Hundertmark C et al (2009) Quantitative phosphokinome analysis of the Met pathway activated by the invasin internalin B from *Listeria monocytogenes*. *Mol Cell Proteomics* 8:2778–2795
44. Roig J, Groen A, Caldwell J et al (2005) Active Nercc1 protein kinase concentrates at centrosomes early in mitosis and is necessary for proper spindle assembly. *Mol Biol Cell* 16:4827–4840
45. Roig J, Mikhailov A, Belham C et al (2002) Nercc1, a mammalian NIMA-family kinase, binds the Ran GTPase and regulates mitotic progression. *Genes Dev* 16:1640–1658
46. Sabarth N, Lamer S, Zimny-Arndt U et al (2002) Identification of surface proteins of *Helicobacter pylori* by selective biotinylation, affinity purification, and two-dimensional gel electrophoresis. *J Biol Chem* 277:27896–27902
47. Salaun L, Linz B, Suerbaum S et al (2004) The diversity within an expanded and redefined repertoire of phase-variable genes in *Helicobacter pylori*. *Microbiology* 150:817–830

48. Schallus T, Jaechk C, Feher K et al (2008) Malectin: a novel carbohydrate-binding protein of the endoplasmic reticulum and a candidate player in the early steps of protein N-glycosylation. *Mol Biol Cell* 19:3404–3414
49. Shin BK, Wang H, Yim AM et al (2003) Global profiling of the cell surface proteome of cancer cells uncovers an abundance of proteins with chaperone function. *J Biol Chem* 278:7607–7616
50. Sinclair JF, O'Brien AD (2002) Cell surface-localized nucleolin is a eukaryotic receptor for the adhesin intimin-gamma of enterohemorrhagic *Escherichia coli* O157:H7. *J Biol Chem* 277:2876–2885
51. Sinclair JF, O'Brien AD (2004) Intimin types alpha, beta, and gamma bind to nucleolin with equivalent affinity but lower avidity than to the translocated intimin receptor. *J Biol Chem* 279:33751–33758
52. Watanabe K, Tachibana M, Kim S et al (2009) EEVD motif of heat shock cognate protein 70 contributes to bacterial uptake by trophoblast giant cells. *J Biomed Sci* 16:113
53. Watanabe T, Hirano K, Takahashi A et al (2010) Nucleolin on the cell surface as a new molecular target for gastric cancer treatment. *Biol Pharm Bull* 33:796–803
54. Watanabe T, Tsuge H, Imagawa T et al (2010) Nucleolin as cell surface receptor for tumor necrosis factor-alpha inducing protein: a carcinogenic factor of *Helicobacter pylori*. *J Cancer Res Clin Oncol* 136:911–921
55. Weber SS, Ragaz C, Hilbi H (2009) The inositol polyphosphate 5-phosphatase OCRL1 restricts intracellular growth of *Legionella*, localizes to the replicative vacuole and binds to the bacterial effector LpnE. *Cell Microbiol* 11:442–460
56. Wilkinson KD (2004) Quantitative analysis of protein–protein interactions. *Methods Mol Biol* 261:15–32
57. Wood LD, Irvin BJ, Nucifora G et al (2003) Small ubiquitin-like modifier conjugation regulates nuclear export of TEL, a putative tumor suppressor. *Proc Natl Acad Sci USA* 100:3257–3262